

Material-dependent Ultrasonic Heating Behavior during the Reshaping of Dry Paper Webs

André Hofmann,^{a,*} Albrecht Löwe,^a and Marek Hauptmann^b

The use of ultrasonic tools during the reshaping of dry paper webs results in a temperature increase. This work aimed to determine the influence of the material and the ultrasonic process parameters of amplitude, ultrasonic duration, and static process pressure on the heating behavior of paperboard during ultrasonic-assisted reshaping. The results showed that the initial process pressure, the ultrasonic amplitude, and the compression resistance of the material noticeably influenced the heating rate. Materials with low compression resistance tended to reach higher initial heating rates during ultrasonic treatment. In addition, coating the paperboard led to an even temperature distribution in the paperboard during the ultrasonic process.

Keywords: Ultrasound; Forming; Paperboard; Material heating

Contact information: a: Chair of Processing Machines and Processing Technology, Technische Universität Dresden, Bergstraße 120, 01069 Dresden, Germany; b: Chair of Packaging Machines and Packaging Technology, Steinbeis Hochschule Berlin, 12489 Berlin, Germany;

* Corresponding author: andre.hofmann1@tu-dresden.de

INTRODUCTION

The reshaping of dry paperboard is a sensible alternative to the thermoforming of plastics to produce cups, cans, or trays. In recent years, the connections between the material and process parameters and quality in forming paperboard by deep-drawing have been extensively investigated. Specific heating of the material (Hauptmann and Majschak 2011) and a controlled blank holder force (Hauptmann *et al.* 2016) can lead to a noticeable increase in forming degree and forming quality. The main forming parameters (blank holder force and forming temperature) also influence the elongation of the material in the forming process. According to Hofmann *et al.* (2019), the maximum elongation of the material decreases by up to 30% with increasing forming temperature. Accordingly, low process temperatures can provide high material elongation, which result in a high risk of cracks during the forming process.

However, further development of forming technology with ultrasonic tools promises increased process and forming quality. According to Löwe *et al.* (2017), the required forming force can be reduced up to 80% by using ultrasonic tools. In addition, the use of vibrating tools results in increased material densification. Hofmann and Hauptmann (2020) achieved a maximum material densification of approximately 30% by using ultrasonic tools. Due to the additional dynamic material compression, the characteristic wrinkles of deep drawing were strongly compressed, which increased the surface smoothness and the stability of the formed parts (Löwe *et al.* 2017).

In addition to the mechanical strain on the paperboard during the ultrasonic-assisted reshaping process, a noticeable increase in the material temperature occurs. Löwe *et al.* (2017) report that the increase in material temperature is mainly dependent on the ultrasonic amplitude and the direction of vibration. The temperature change depends on the

type of acting forces (compressive, tensile, or shear force) and the material properties. In the literature, the mechanisms of energy conversion that occur in the ultrasonic-assisted reshaping of paper are not described in detail. However, there is a great knowledge of energy conversion mechanisms in the welding and sealing of thermoplastic and metallic materials with ultrasonic tools. The energy conversion for ultrasonic-assisted joining thermoplastics is based on the two mechanisms of interfacial friction (Tolunay *et al.* 1983; Hongoh *et al.* 2006) and internal friction (Chernyak 1973). Zhang *et al.* (2010) found that, until the glass transition temperature was reached, interfacial friction was the mainly occurring phenomenon. Further heating above the glass transition temperature was caused by intermolecular friction. According to Neumann *et al.* (2017), the heating above the glass transition temperature is mainly influenced by ultrasonic amplitude.

Based on the findings on the heating mechanisms of synthetic polymers, the temperature increase during the ultrasonic volume gentle smoothing of paper was investigated (Wanske 2010). In the case of parallel oscillations to the material surface, only very small deformation amplitudes or shear rates act inside the material. Due to the interfacial friction between the paperboard and the ultrasonic tool, the paperboard heats up from the outside to the inside, depending on the coefficient of friction of the material surface (Wanske 2010; Löwe *et al.* 2019). Internal friction occurs mainly in the orthogonal direction of vibration to the material surface, where the material heats up from the inside to the outside due to pressure cycling stress. During the orthogonal ultrasonic oscillation direction, a parallel ultrasonic oscillation direction also occurs due to the transverse contraction of the ultrasonic tools. However, the ultrasonic amplitude of the parallel oscillation direction is less than 5% of the ultrasonic amplitude of the orthogonal oscillation direction. For the load case of an orthogonal ultrasonic oscillation direction (as occurs during ultrasonic reshaping under the blank holder), the interfacial friction between the sonotrode and paper material can be ignored. Löwe *et al.* (2019) investigated vertical oscillations directed at the paperboard surface and the basic relationships between the ultrasonic parameters of amplitude and contact pressure and paperboard heating. The heating of the material was shown to increase with increasing contact pressure, and the measured maximum temperatures of the parallel oscillation were about two times higher than those of the vertical oscillation, whereby the material heats up faster with the vertical oscillation direction. The ultrasonic amplitude has only a minor influence on the heating of the paperboard when the direction of oscillation is vertical (Löwe *et al.* 2019).

However, the influence of materials with different mechanical properties that influence material heating during gap-controlled ultrasonic forming has not yet been investigated. This work investigated the material properties in the heating of paperboard during ultrasonic forming to find a relationship between these material properties, the ultrasonic parameters, and the heating behavior of paperboard materials. Furthermore, it is possible to determine material properties that influence the heating behavior of the material in the ultrasonic process. Therefore, materials with a lower combustion tendency in the ultrasonic embossing process can be selected for the refinement of packaging.

EXPERIMENTAL

Materials and Measurements

All the experiments were performed at $23\text{ °C} \pm 1\text{ °C}$ with an air humidity of $50\% \pm 2\%$, and each material was air-conditioned for at least 24 h before the examination. The resulting material moisture content for the selected paperboards is listed in Table 1. After

the 24 h conditioning period, the experiments occurred under the same climatic conditions. The cardboard was cut then into samples with a width of 15 mm and a length of 150 mm. To investigate material-dependent heating during ultrasonic forming, six conventional paperboard materials were selected. The compositions of the materials are shown in Fig. 1. Material 1 (Trayforma Natura) and material 2 (Trayforma Ensocard), provided by Stora Enso (Imatra, Finland), were untreated raw materials without any functionalization on the surface. Compared to the first two materials, material 3 (Trayforma Ensocoat) (Stora Enso, Imatra, Finland) had a double-coated surface and a single-coated paperboard backside. The chemical structure of the single material layers was identical to those of the first two materials. In contrast to material 3, material 4 (Trayforma Tambrite) (Stora Enso, Imatra, Finland) had a middle layer of thermo-mechanical wood pulp (TMP) and a surface sizing of the paperboard backside. Material 5 (Trayforma Performa Bright) (Stora Enso, Imatra, Finland) had a triple coating of the material surface and a middle layer of thermo-chemical mechanical wood pulp (CTMP). Otherwise the composition was similar to that of material 4. Material 6 (Incada Exel) (Iggesund Paperboard AB, Iggesund, Sweden) had the same composition as material 4 aside from the surface sizing on the paperboard backside.

Material 1	Material 2	Material 3	Material 4	Material 5	Material 6
Cellulose	Cellulose	Double-coated	Double-coated	Triple-coated	Double-coated
Cellulose/CTMP	Cellulose/CTMP	Cellulose	Cellulose	Cellulose	Cellulose
Cellulose	Cellulose	Cellulose/CTMP	TMP	CTMP	TMP
		Cellulose	Cellulose	Cellulose	Cellulose
		Single-coated	Surface sizing	Surface sizing	

Fig. 1. The compositions of the paperboard materials used

All of the used materials had approximately the same grammage but differed in their properties because of their internal structure. The characteristic material values and the material properties of heating during ultrasonic forming (*e.g.*, embossing) are listed in Table 1. The thickness reduction under compressive load depends on the compression resistance of the material. According to test standard DIN 55440-1 (1991), the compression force and the corresponding compression path were determined. The maximum relative material compression of the materials was between 33% and 62%. To allow comparison of the materials, a compression work ($W_{30\%}$) with a relative material compression of 30% was used. The specific volume is the quotient of the material thickness and the grammage. A high specific volume indicated a large pore volume of the paper material, which resulted in a low compression resistance of the material. The specific volume was determined by the process parameters, the fiber composition, and the use of additives during the production of the paperboard material. In the present study, the specific volume was used as an indicator of the pore volume of commercially available paperboard materials. According to Hauptmann *et al.* (2015), the tensile strength and the bending resistance determined the forming ability of the paperboards, and they were also influenced by the material composition. Generally, materials with a high cellulose content in the fiber network and a low specific volume tended to have high tensile strength and bending resistance. Compared to chemically pulped cellulose fibers, TMP and CTMP fibers usually had higher fiber stiffness and lower cross-linking capacity in the fiber network. Depending on the mass fraction and the manufacturing parameters, paperboards with TMP and CTMP fibers usually had a higher specific volume, lower tensile strength, and lower bending

resistance. The mass fraction of the fibers used and the manufacturing parameters of commercially available paperboards was unknown and could not be determined even with conventional non-destructive measuring methods. But the materials were categorized according to their properties as follows. Materials 1 and 2 had the same composition without a surface coating. They differed only in their properties. Compared with material 2, material 1 had a lower bending resistance and a higher tensile strength. The same applied to material 4 and material 6. Therefore, the influence of bending resistance and tensile strength can be investigated for uncoated materials (M1, M2) and for coated materials (M4, M6). The influence of a surface coating can be investigated by comparing the heating behavior between material 3 and material 1 or material 2. At the same time, the influence of the middle layer could be investigated by comparing the heating behavior between material 5 and material 4 and/or 6.

Table 1. Material Characterization

Material	1	2	3	4	5	6
Grammage (g/m ²)	350	330	330	310	320	325
Material Thickness (μm)	450	415	450	600	560	590
Material Moisture Content (%)	7.5	7.5	6.8	8.7	8.5	8.2
Specific Volume (cm ³ /g)	1.285	1.257	1.363	1.935	1.75	1.815
Compression Work W_{30%} (mJ)	1.302	1.087	1.495	0.285	0.435	0.35
Bending resistance (Nm)						
MD	620	690	640	260	310	790
CD	1160	1270	1130	530	480	1310
Tensile strength (N/mm)						
MD	28.2	22.6	24.4	17.3	16.7	11.8
CD	13.1	11.0	11.6	7.9	8.1	6.9

Test Equipment

Analysis of the heating behavior of paper during ultrasonic-assisted forming was conducted on a gap-controlled test module. The gap-controlled test module for ultrasonic forming of paper was described in detail by Hofmann and Hauptmann (2020). A schematic representation of the test equipment is shown in Fig. 2a. A special feature of the experimental setup is that the adjusted distance (tool gap) between the sonotrode and the anvil remains constant during the ultrasonic treatment of the paperboard. Depending on the compression properties of the paperboard, the initial process pressure (P_{int}) was set via the tool gap. P_{int} was calculated with the help of force measurements taken with a quartz crystal force sensor (Quarzkristallkraftsensor 9213B, Kistler, Sindelfingen, Germany). For the following experiments, the sonotrode was pressed into the back of the prepared paperboard samples until the initial process pressure was reached. As a result of the acting static process pressure, the material in the tool gap was statically densified. After the initial process pressure was set, the ultrasonic oscillation switched on. Therefore, the sonotrode started to oscillate and the material in the tool gap was exposed to ultrasonic oscillation. The sonotrode with a width of 15 mm and a length of 100 mm had a total electrical output of 2300 W and maximum vibration amplitude of 55 μm. During the ultrasonic treatment, there was a decrease of the material thickness in the constant tool gap as a consequence of the introduced ultrasonic amplitude and the resulting dynamic densification of the material (Hofmann and Hauptmann 2020). Due to the constant tool gap, the initial process pressure decreases with the ultrasonic duration depending on the compression properties of the paperboard. With the experimental setup, the process parameters of ultrasonic amplitude

and ultrasonic duration could also varied. In the experiments, an initial process pressure of up to 2.5 MPa, a maximum ultrasonic amplitude of $50 \mu\text{m} \pm 1 \mu\text{m}$, and an ultrasonic duration of 1 s were achieved. A summary of the parameter settings for the investigation of the material-dependent heating behavior during the reshaping of paperboard is given in Table 2. To elucidate the relationships between the process parameters, the material properties, and the heating behavior during ultrasonic reshaping, a full factorial experimental design was prepared. The full factorial experimental design consisted of 81 test points for each material, each of which was repeated five times to ensure statistically safe results.

Table 2. Parameter Levels for the Experiments

Parameter	Settings								
Initial Process Pressure (MPa)	0.05	0.15	0.3	0.6	0.75	1	1.5	2	2.5
Ultrasonic Amplitude (μm)	15			30			50		
Ultrasonic Duration (sec)	0.25			0.5			1		

To determine the heating behavior of the paperboard samples during the ultrasonic process, a Variotherm infrared thermography system (InfraTec GmbH, Dresden, Germany) with a macro infrared lens was used. This system allowed a resolution of $10 \mu\text{m}$ per pixel with a measuring range of $256 \text{ pixels} \times 256 \text{ pixels}$ and a scanning frequency of 100 Hz. Figure 2a shows the system used to measure the heating behavior. The infrared camera was placed perpendicular to the material thickness direction (z-direction) to measure temperature change within the material at the tool gap during the ultrasonic treatment. Validation of the measured temperature values was carried out using electrical thermocouples that were placed in the focus of the camera. Figure 2b shows the validation of the material temperatures measured *via* the infrared camera system. For a temperature range of $20 \text{ }^\circ\text{C}$ to $230 \text{ }^\circ\text{C}$, the measurements from the infrared camera matched closely with the measurements of the thermocouples. At temperatures above $230 \text{ }^\circ\text{C}$, the temperature measured by the infrared system differed noticeably from the measurement recorded by the thermocouples.

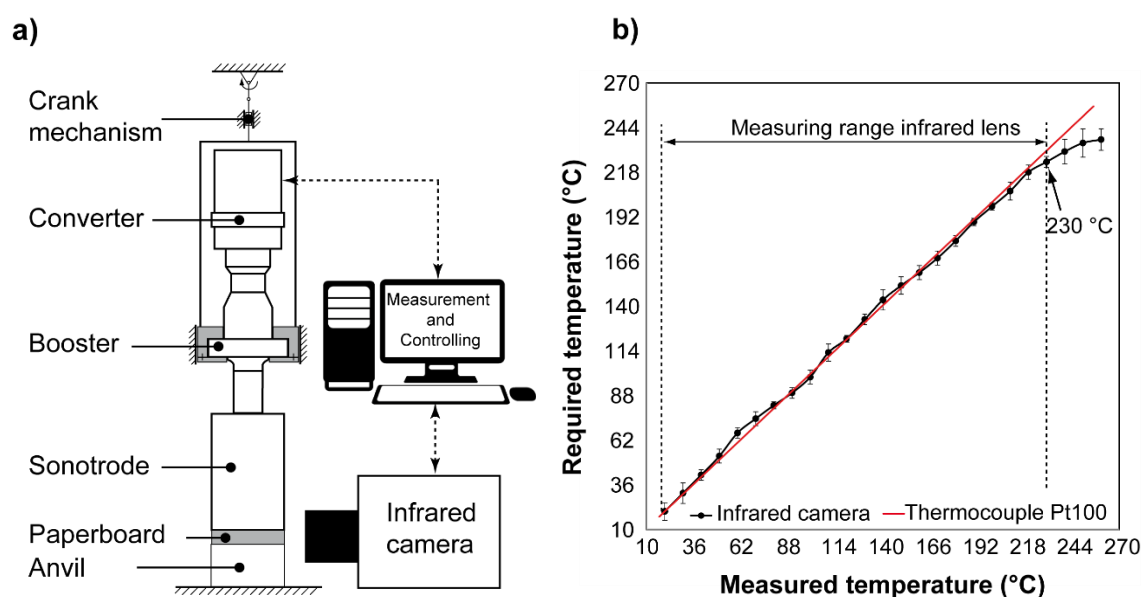


Fig. 2. The measurement setup for infrared thermography (a); validation of the infrared measuring system for materials 1 to 6 (b)

RESULTS AND DISCUSSION

Due to the ultrasonic vibrations of the upper embossing tool (sonotrode), the material was heated during the reshaping of paperboard. The initiation of the ultrasonic longitudinal oscillation into the material was performed perpendicular to the material surface. Because of the ultrasonic amplitude, heating from the inside to the surface of the material was achieved. Figure 3 shows the temperature changes in the ultrasound-assisted, gap-controlled reshaping of dry paperboard. At the beginning of the ultrasonic process, high initial heating rates (HR) were achieved that caused a rapid increase in the process temperature inside the material, which was similar to the force-controlled investigations by Löwe *et al.* (2019) and Wanske (2010). The initial heating rate was defined as the difference between the material temperature at the beginning of the ultrasonic process and the material temperature after an ultrasonic duration of 200 ms. As ultrasonic treatment progressed, the initial heating rate reduced, and a temperature plateau formed. The maximum material temperature (T_{max}) was the upper limit, and 90% of the maximum material temperature (T_{90}) was the lower limit of the plateau.

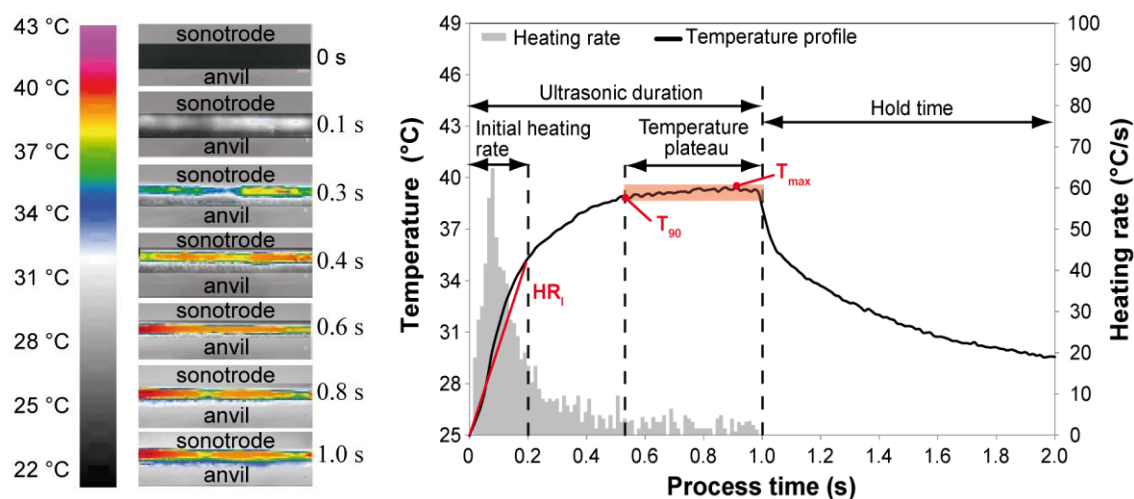


Fig. 3. The heating behavior in the ultrasound-assisted, gap-controlled reshaping of paperboard based on the example of material M1

The reduction in the heating rate was caused by the dynamic densification of the material in the tool gap (Hofmann and Hauptmann 2020). A reduction in thickness occurred mainly in the first 300 ms due to additional dynamic material densification during ultrasonic reshaping. In contrast with the material thickness, the tool gap in the reshaping process remained constant, which caused the process pressure to decrease with increasing ultrasonic duration. Due to the material compression, the effective ultrasonic amplitude was reduced, which resulted in reduced pressure cycling stress in the material. Lower pressure cycling stresses in the material produced lower dynamic material compressions and lower internal friction losses, which reduced the initial heating rate and the material temperature.

The amount of force drop at the beginning of the ultrasonic process, the associated initial heating rate, and the maximum process temperature depended on the compression properties of the paperboard material and the initial process pressure at the beginning of the ultrasonic duration. Materials with low compression resistance achieved high dynamic material densifications with a low elastic compression portion during the ultrasonic process. Figure 4a shows the relationship between the initial heating rate and the dynamic

material densification during the ultrasonic process. A high material densification together with a low elastic deformation portion in the ultrasonic process led to a high initial heating rate. Depending on the material compression properties, the initial heating rate and the material densification decreased with the ultrasonic duration. Figure 4b shows the heating rate over the ultrasonic duration for materials M1 to M6 with an initial process pressure of 1 MPa and an ultrasonic amplitude of 30 μm . Materials M4, M5, and M6 had a lower compression resistance than materials M1, M2, and M3. In addition, materials M4, M5, and M6 showed a high initial heating rate at the beginning of the ultrasonic duration, up to approximately 150 ms. In contrast, materials M1, M2, and M3 showed a noticeably lower initial heating rate at the beginning of the ultrasonic process, which decreased slightly with increasing ultrasonic duration. Due to the different compression resistances of the materials, various tool gap settings occurred with an initial process pressure of 1 MPa. Consequently, materials with a lower compression resistance resulted in a smaller tool gap. Therefore, the ratio of effective ultrasonic amplitude to tool gap was greater than for materials with a high compression resistance. During the ultrasonic treatment, high effective ultrasonic amplitudes led to large dynamic material densifications and internal friction losses. As a result, materials with low compression resistance achieved high initial heating rates during the ultrasonic process.

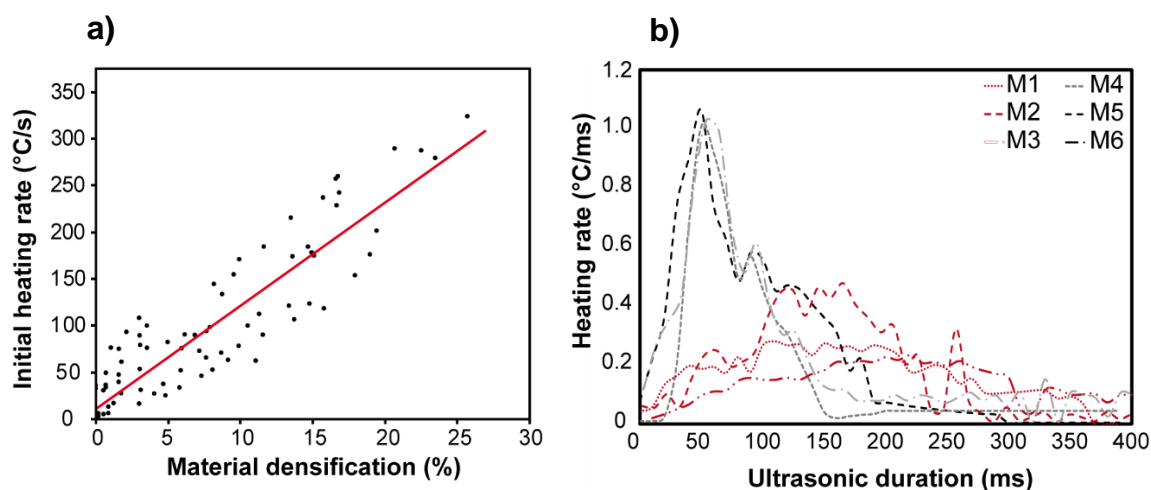


Fig. 4. The relationship between heating rate and material densification (a); Dependence of the heating rate on the ultrasonic duration for materials 1 to 6 at 2 MPa and an ultrasonic amplitude of 30 μm (b)

Accordingly, the low initial heating rates for materials with high compression resistance resulted from the low ratio of effective ultrasonic amplitude to material thickness in the tool gap. Low effective ultrasonic amplitudes led to a lower dynamic material densification in the ultrasonic process, which is why the heating rate was more constant and decreased slightly over the ultrasonic duration. In addition, lower alternating pressure stresses and thus internal friction losses were generated, which resulted in comparatively moderate initial heating rates. Furthermore, materials with a low specific volume showed a high compression resistance, whereby a large part of the deformation in the ultrasonic process was reversible. High reversible or elastic deformations lead to lower dynamic material densification, which is why materials with a high compression resistance tend to achieve lower initial heating rates. Another effect of the compression properties in gap-controlled ultrasonic reshaping of paperboard was shown by comparing the material heating behavior. Figure 5 shows the relationship between the initial heating rate and the process parameters of ultrasonic amplitude and process pressure for materials with low and

high compression resistance. The paperboards M1, M2, and M3 achieved low initial heating rates based on the high compression resistance and the low specific volume. The increase of the static process pressure was achieved by reducing the tool gap between sonotrode and anvil. Therefore, an increasing process pressure reduces the specific volume of the paperboard. According to Hofmann and Hauptmann (2020), low specific volumes resulted in low dynamic material densification with a high elastic compaction ratio. As a result, lower initial heating rates were achieved in the ultrasonic process. By increasing the amplitude, the ratio of the effective amplitude to the material thickness in the tool gap was increased. Thus, high amplitudes led to greater dynamic material densification and initial heating rates. However, for the paperboards M4, M5, and M6 with a high specific volume it was found that the initial heating rate increases with the increase of the static process pressure. Materials with high specific volumes achieved low dynamic material densification with low elastic compression portion at low static process pressures and amplitudes. With the increase of the static process pressure up to 2.5 MPa, the dynamic material densification and the ratio of the effective amplitude to the material thickness in the tool gap also increased. At the same time, there was a comparatively small increase in the elastic compression portion in contrast to the materials M1, M2, and M3. Furthermore, the decrease in the initial heating rate with increasing material density could be attributed to the decrease in thermal diffusivity. According to Zhao and Schabel (2012), paperboard materials with lower porosity or high material density showed a noticeably lower thermal diffusivity than materials with high porosity. Therefore, materials M1, M2, and M3, which had a comparatively low specific volume, showed noticeably lower initial heating rates. They achieved their highest initial heating rates at low initial process pressures, the maximum of which was 0.3 MPa. In contrast, materials M4, M5, and M6, which had a large specific volume, showed the highest initial heating rates and had a maximum process pressure of 2.5 MPa. For the paperboards, M4, M5, and M6, a further increase in static process pressure above 2.5 MPa should lead to a further increase in the elastic deformation portion, whereby the initial heating rate decreases after reaching its maximum. An increase in process pressure above 2.5 MPa could not be achieved with the applied measuring method and measuring equipment.

Figure 5 shows that the ultrasonic amplitude also influenced the initial heating rate. Regardless of material properties, an increase in the ultrasonic amplitude led to an increase in the initial heating rate. This occurred because larger amplitudes within the tool gap produced higher dynamic material densifications and internal friction losses.

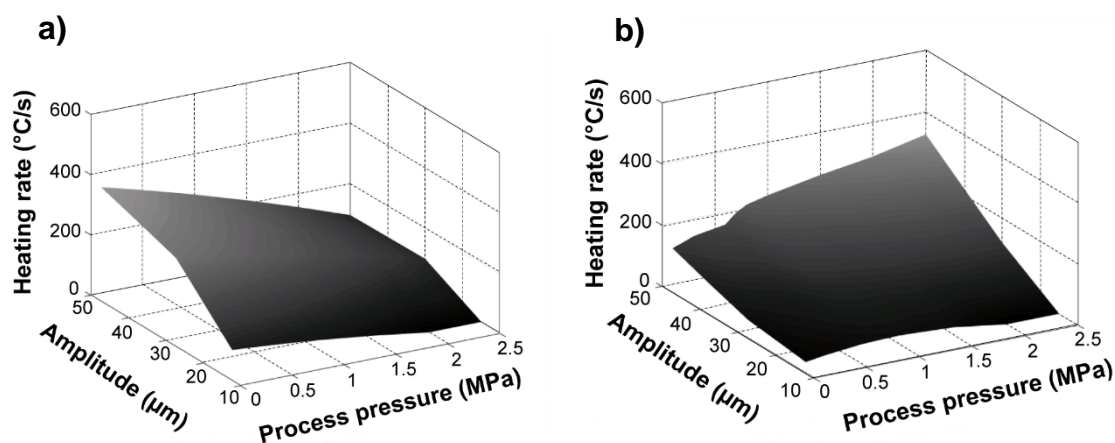


Fig. 5. The heating behavior in the ultrasonic process for material M2 (a) with a high compression resistance and material M4 (b) with a low compression resistance

However, there was also an interaction of the amplitude with the initial process pressure, which was dependent on the compression properties of the material used. For materials M1, M2, and M3, which had high compression resistance, the influence of the ultrasonic amplitude decreased with increasing initial process pressure. However, the influence of the ultrasonic amplitude increased with increasing initial process pressure for materials M4, M5, and M6, which had low compression resistance.

The temperature development in the gap-controlled ultrasonic-assisted reshaping process had a direct connection with the initial heating rate. Figure 6a shows the general relationship between the initial heating rate and the maximum material temperature for an ultrasonic duration of 200 ms. The same relationships between initial heating rate and the process parameters of amplitude and between initial process pressure and the compression properties of the material applied to the maximum process temperature. In general, high initial heating rates produced high maximum material temperatures. However, Fig. 6 shows a noticeable variation in the process temperature at the same heating rate. Depending on the compaction state of the material during the ultrasonic process, there were different maximum process temperatures for the same heating rate. At the same time, Fig. 6b shows an interaction between the initial process pressure and the compression resistance of the material. Consequently, materials with a high compression resistance achieved higher maximum process temperatures at low initial process pressures than materials with a lower compression resistance. Paperboards with a high compression resistance had a high fiber density or a low specific volume. According to Hofmann and Hauptmann (2020), materials with high fiber densities tend to experience low dynamic material densification during the ultrasonic process. The increase of the initial process pressure reduces the tool gap, which increases the fiber density by reducing the pore volume. At the same time, the compression resistance of the material increases, which results in an increase in the elastic portion of the dynamic material compression due to the ultrasonic amplitude. Consequently, high elastic portion of the dynamic material compressions led to lower heating rates in the paperboard.

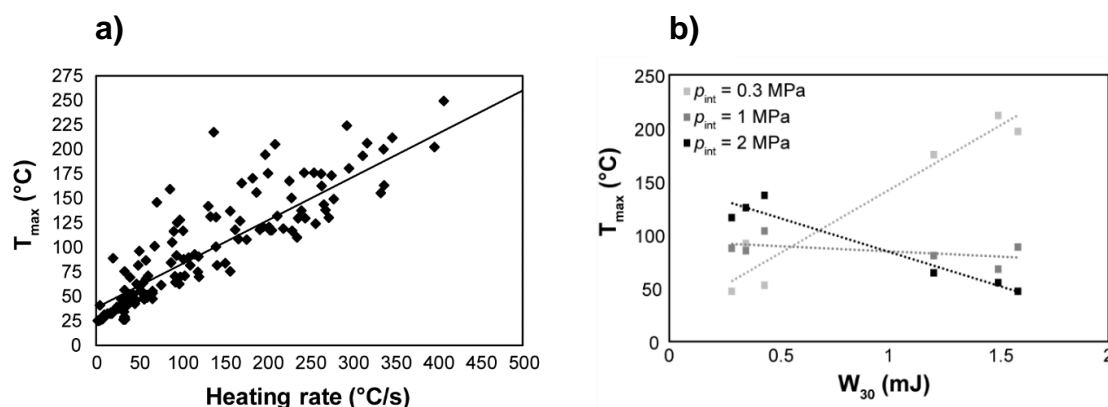


Fig. 6. Relationship between the maximum T_{max} , the initial heating rate (a), and the compression resistance of the material (W_{30}) for different ρ_{int} and an ultrasonic amplitude of 30 μm (b)

In addition, the maximum process temperature was influenced by the ultrasonic duration. Figure 7a shows the relationship between the heating behavior of the materials used and the ultrasonic duration with an initial process pressure of 1 MPa and an ultrasonic amplitude of 30 μm . The paperboard materials M4, M5, and M6 with a low-pressure resistance showed a rapid increase of T_{max} compared to the materials with a high compression resistance. They reached the maximum process temperature with comparatively short ultrasonic durations of 100 ms to 150 ms. But M5 achieved a higher T_{max} compared to M4, and M6. The heating occurred from the inside to the outside

of the material. This means that the middle layer of the paperboard influences energy transformation. In contrast to M4 and M6, the material M5 has a middle layer of CTMP fibers, which leads to a higher thermal energy transformation compared to a middle layer of TMP fibers. In contrast, the materials M1, M2, and M3 showed a noticeably slower increase in material temperature, but they achieved the same temperature level after an ultrasonic duration of approximately 250 ms. Due to inhomogeneous material heating, the initial heating rate was defined as the temperature rise within 200 ms. For ultrasonic durations greater than 200 ms, high material temperatures were achieved even with a low heating rate. Therefore, the relationship between the initial heating rate and the maximum measured process temperature was only valid for an ultrasonic duration of 200 ms.

Furthermore, based on the results, no considerable influence of tensile strength and bending resistance on the heating behavior of the paperboards were observed. Material M1 and M2, as well as materials M4 and M6, showed similar heating behavior with comparable initial heating rates and T_{\max} . At the same time, the heating behavior of M5 and M4 differed despite similar mechanical properties. Therefore, the mechanical properties of tensile strength and bending resistance cannot be used to predict the suitability of the paperboards or to characterize the heating behavior in the ultrasonic-assisted forming process.

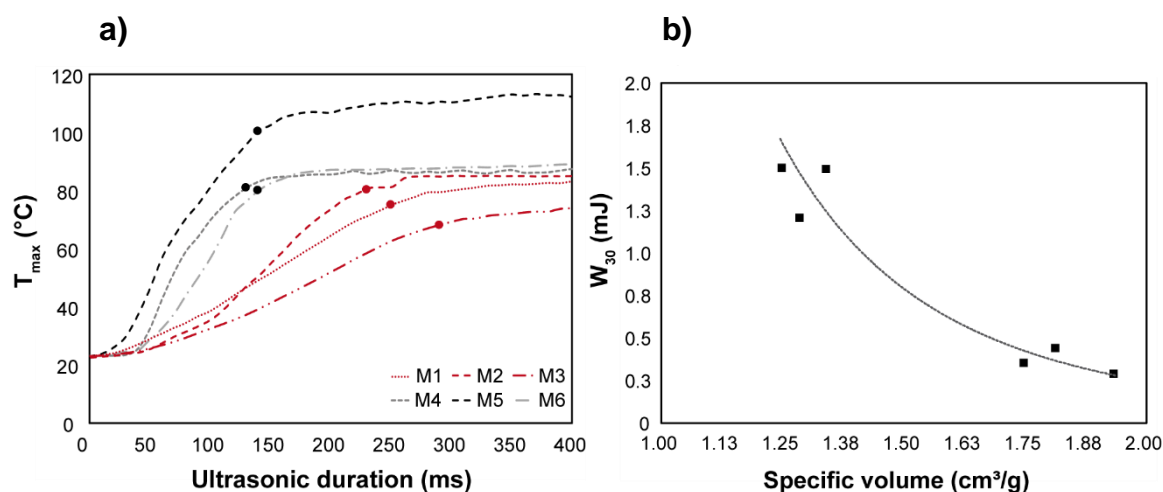


Fig. 7. The heating behavior of various paperboard materials during the ultrasonic reshaping process for an initial process pressure of 1 MPa and an ultrasonic amplitude of 30 μm (a), and the relationship between the compression work and specific volume of paperboard materials (b)

In general, the results indicated that the level of the initial heating rate and the maximum temperature was dependent on the process parameters of the ultrasonic amplitude, the process pressure, and the compression properties of the material. The specific volume is a property of the material, which results from the ratio of the thickness of the material to the grammage and indirectly provides information about the compression properties (*e.g.*, compression resistance) of a paperboard. The relationship between the compression work and the specific volume is described in Table 1 and illustrated in Fig. 7b. Materials with low compression resistance had a high specific volume, and high specific volumes led to high initial heating rates during the ultrasonic treatment. The maximum temperature depended on the material characteristics of the specific volume and the associated dynamic compression in the ultrasonic process. At short ultrasonic durations, materials with high specific volumes had higher maximum temperatures than materials with low specific volumes at short ultrasonic durations. In addition, materials with a lower specific volume indicated a tendency to lower T_{\max} in the ultrasonic process.

The coating of the paperboard influenced the specific volume considerably. Multiple coated materials showed comparatively low specific volumes with high compression resistance. Therefore, the influence of the coating of a paperboard on the heating behavior was investigated. The heating behavior of material M1 was compared with that of material M3. Materials M1 and M3 had similar layer composition, specific volume, and compression resistance. However, material M3 had a double coating on the upper side and a single coating on the underside, but material M1 had no coating. To compare heating behavior, both materials were treated with two ultrasonic amplitudes of 30 μm and 50 μm , an ultrasonic duration of 1000 ms, and a contact pressure of 1 MPa. The results of the investigations are shown in Fig. 8. No noticeable differences in initial heating rate and maximum process temperature were observed. However, the combustion of M3, a coated material, with an ultrasonic amplitude of 50 μm showed a considerably homogeneous distribution. For material M1, which was not coated, areas with a high degree of combustion were formed, and other areas were less burned. Because of the manufacturing process, the paperboard had an inhomogeneous pulp density, which caused local compressive stress peaks during the ultrasonic treatment of uncoated papers and inhomogeneous combustion. Because of the coating on the paperboard, the surface of the material was homogenized, and the process pressure was uniformly introduced into the material. Homogeneous pressure distribution resulted in uniform heating of the paperboard, which reduced the amount of material combustion during ultrasonic treatment.

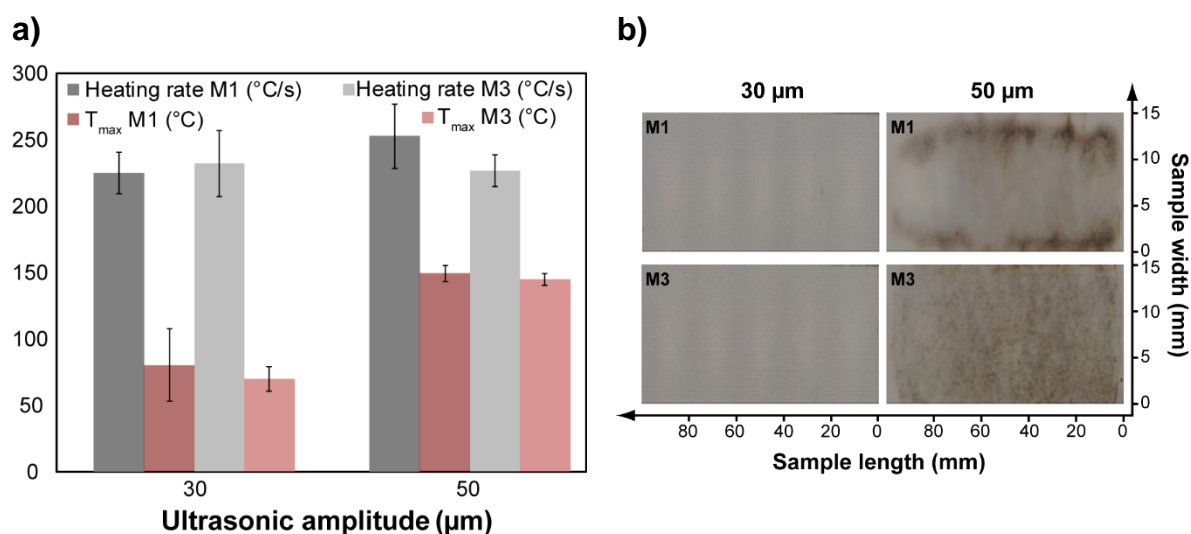


Fig. 8. The influence of coating on the heating behavior of paperboard during ultrasonic treatment with a static contact pressure of 1 MPa and an ultrasonic duration of 1000 ms (a) and the combustion characteristics depending on the surface coating

CONCLUSIONS

1. Compression resistance and specific volume were used to examine the heating behavior of paperboard during the ultrasonic process. Materials with high specific volumes or a low-pressure resistance showed high initial heating rates with increasing initial process pressure.
2. Materials with low-pressure resistance showed high initial heating rates at the beginning of ultrasonic-assisted paperboard reshaping, which led to a rapid increase in

the process temperature inside the material. During the ultrasonic treatment, the heating rate was reduced, which could be attributed to the dynamic material densification inside the tool gap.

3. High dynamic material densification during the ultrasonic process led to high initial heating rates, which strongly decreased as ultrasonic duration increased. Due to high material densification, the alternating pressure stresses in the tool gap were reduced, which reduced the internal friction losses, and the paperboard heated up less quickly.
4. For paperboard materials with a high compression resistance, the heating rate decreased as the initial process pressure increased. The increase of the initial process pressure led to a high dynamic-elastic deformation in the ultrasonic process, which reduced the internal friction losses and thus the heating rate.
5. The coating of the material led to a more homogeneous heating of the paperboard than uncoated materials. With the coating of the material, a leveling of the surface roughness was achieved, which resulted in a higher surface smoothness. With the increase of the surface smoothness, a homogeneous pressure distribution between sonotrode and material was achieved that resulted in uniform heating of the paperboard.

ACKNOWLEDGMENTS

The authors thank the German Federation of Industrial Research Association (AiF) and the German Federal Ministry for Economic Affairs and Energy (BMWi) for providing financial support (Project 19717 BR). Open Access Funding was provided by the Publication Fund of the TU Dresden

REFERENCES CITED

- Chernyak, B. Y. (1973). "The process of heat formation in the ultrasonic welding of plastics," *Welding Production* 8, 87-91.
- DIN 55440-1 (1991). "Packaging test - compression test - test with a constant conveyance-speed," German Institute for Standardization, Berlin, Germany.
- Hauptmann, M., and Majschak, J.-P. (2011). "New quality level of packaging components from paperboard through technology improvement in 3D forming," *Packaging Technology and Science* 24(7), 419-439. DOI: 10.1002/pts.941
- Hauptmann, M., Wallmeier, M., Erhard, K., Zelm, R., Majschak, J.-P. (2015). "The role of material composition, fiber properties and deformation mechanisms in the deep drawing of paperboard," *Cellulose* 22, 3377-3395. DOI: 10.1007/s10570-015-0732-x
- Hauptmann, M., Weyhe, J., and Majschak, J. P. (2016). "Optimisation of deep drawn paperboard structures by adaptation of the blank holder force trajectory," *Journal of Materials Processing Technology* 232, 142-152. DOI: 10.1016/j.jmatprotec.2016.02.007
- Hofmann, A., and Hauptmann, M. (2020). "Ultrasonic induced material compression during the gap-controlled reshaping of dry paper webs by embossing or deep drawing," *BioResources* 15(2), 2326-2338. DOI: 10.15376/biores.15.2.2326-2338
- Hofmann, A., Wallmeier, M., Hauptmann, M., and Majschak, J.-P. (2019). "Characterization of the material elongation in the deep drawing of paperboard," *Packaging Technology and Science* 32(6), 287-296. DOI: 10.1002/pts.2436

- Hongoh, B., Miura, H., Ueoka, T., and Tsujino, J. (2006). "Temperature rise and welding characteristics of various frequency ultrasonic plastic welding systems," *Japanese Journal of Applied Physics* 45(5B), 4806-4811. DOI: 10.1143/JJAP.45.4806
- Löwe, A., Hauptmann, M., and Majschak, J. P. (2017). "The effect of ultrasonic oscillation on the quality of 3D shapes during deep-drawing of paperboard," *BioResources* 12(4), 7178-7194. DOI: 10.15376/biores.12.4.7178-7194
- Löwe, A., Hauptmann, M., Hofmann, A., and Majschak, J.-P. (2019). "Temperature development of cardboard in contact with high-frequency vibrating metal surfaces," *Bioresources* 14(2), 3975-3990. DOI: 10.15376/biores.14.2.3975-3990
- Löwe, A., Hofmann, A., and Hauptmann, M. (2017). "The use and application of ultrasonic vibrations in the 3D deformation of paper and cardboard," *Journal of Materials Processing Technology* 240, 23-32. DOI: 10.1016/j.jmatprotec.2016.09.006
- Neumann, U., Mitschang, P., Weimer, C., and Gessler, A. (2017). "Influence of ultrasonic preforming to the mechanical properties of carbon fiber reinforced composites," *Journal of Plastics Technology* 2017(13), 32-66.
- Tolunay, M. N., Dawson, P. R., and Wang, K. K. (1983). "Heating and bonding mechanisms in ultrasonic welding of thermoplastics," *Polymer Engineering & Science* 23(13), 726-733. DOI: 10.1002/pen.760231307
- Wanske, M. (2010). *Hochleistungs-Ultraschallanwendungen in der Papierindustrie: Methoden zur Volumenschonenden Glättung von Oberflächen [High-performance Ultrasound Applications in the Paper Industry: Methods for Volume-smoothing Surfaces]*, Ph.D. Dissertation, Technische Universität Dresden, Dresden, Germany.
- Zhang, Z., Wang, X., Lou, Y., Zhang, Z., and Wang, L. (2010). "Study on heating process of ultrasonic welding for thermoplastics," *Journal of Thermoplastic Composite Material* 23(5), 647-664. DOI: 10.1177/0892705709356493
- Zhao, S., and Schabel, S. (2012). "Modellierung der thermischen Eigenschaften von Papier unter Druckbeanspruchung [Modeling the thermal properties of paper under pressure]," *Wochenblatt für Papierfabrikation* 140(4), 260-264.

Article submitted: March 3, 2020; Peer review completed: April 18, 2020; Revised version received and accepted: May 8, 2020; Published: May 13, 2020.
DOI: 10.15376/biores.15.3.4947-4959